

# Transient Enhancement in Add-on Feedforward Algorithms for High-performance Mechatronic Systems<sup>\*</sup>

Xu Chen<sup>\*</sup> and Masayoshi Tomizuka<sup>\*</sup>

<sup>\*</sup> Department of Mechanical Engineering, University of California, Berkeley, CA, 94720, USA (e-mails: {maxchen,tomizuka}@me.berkeley.edu).

**Abstract:** In this paper, we analyze the problem of control injection in feedforward compensation, and discuss the transient enhancement in add-on feedforward algorithms. In contrast to the common feedforward injection at the plant input, the updated reference feedforward design is discussed with the advantage of accelerated transient. Such a configuration also brings convenience from the viewpoints of filter implementation and uniformed design in industrial mass production. Two implementation examples are provided from advanced manufacturing and precision motion control.

*Keywords:* feedforward control, vibration rejection, iterative learning control, mechatronics

## 1. INTRODUCTION

Combining feedforward and feedback controls is a standard practice in control engineering. This paper discusses the problem of control-effort injection in such a combined control scheme. More specifically, consider a general closed-loop control system in Fig. 1. The dotted lines denote the distribution of the feedforward efforts, which are “added on” to the baseline feedback system. From the viewpoint of injecting the add-on feedforward command, we can classify the two designs as:

- *updated control (UC)*, where feedforward  $u_{ff}$  is directly injected at the input of the plant  $P$ ;
- *updated reference (UR)*, where  $r_{ff}$  is added as an update of the reference  $r$ .

For feedforward control, updated reference is equivalent to control injection at the location of the feedback error  $e$  in Fig. 1. In both cases, the dynamics between  $r_{ff}$  and  $y$  equals the complementary sensitivity function  $T = PC/(1 + PC)$ .

Both UC and UR feedforward control are vastly implemented in practice. Popular examples can be found, for instance, in general two-degree-of-freedom motion control (Sugie and Yoshikawa, 1986; Li and Tomizuka, 1999; Liu et al., 2005), iterative learning control (Amann et al., 1996; Bristow et al., 2006; Moore et al., 2006; Ahn et al., 2007; Mishra, 2009), and adaptive or sensor-based feedforward compensation (Bodson et al., 1994; Zhang et al., 2000; Widrow and Walach, 2007). These schemes are all central in mechatronics and industrial motion control. For designing the feedforward filters, representative techniques include: scalar gain approximation such as the P-type iterative learning control (Saab, 1994; Bristow et al., 2006;

<sup>\*</sup> This work was supported by a research grant from Western Digital Corporation, and by the Computer Mechanics Laboratory (CML) in the Department of Mechanical Engineering, UC Berkeley.

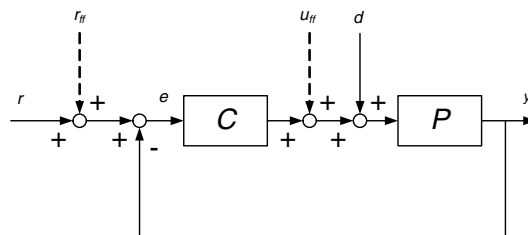


Fig. 1. Two allocations of the feedforward command:  $P$  and  $C$  are respectively the controlled plant and the feedback compensator;  $r$  and  $d$  are the reference and the lumped disturbance

Ahn et al., 2007), discrete-time Taylor expansion (Widrow and Walach, 2007), zero-phase-error-tracking (ZPET) design (Tomizuka, 1987), and  $H_2/H_\infty$  design (Moore et al., 2008; Nie and Horowitz, 2011).

Despite the rich literature about feedforward control and design, not much investigations are available about the difference between UC and UR. From transfer-function analysis, it seems reasonable to always be able to equivalently transform from one scheme to the other, as the structural difference between the feedforward commands in UR and UC is that  $r_{ff}$  in UR is filtered by one additional filter  $C$ . In this paper, further investigations are made to examine the functional differences between UC and UR. We remark first, that transfer-function analysis reveals *the steady-state performance* but not the transient properties of the system. For the class of *add-on* or *plug-in* feedforward control, the transient at different injection points are different. Analysis and solutions of the problem is important for plug-in compensation, which is central in many practical problems such as iterative learning control (where add-on feedforward command is injected to the closed loop at different iterations) and feedforward

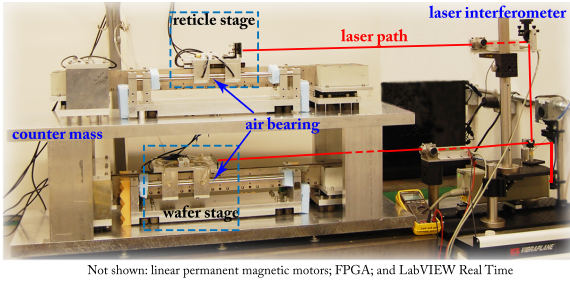


Fig. 2. A testbed of wafer-scanner system for semiconductor manufacturing

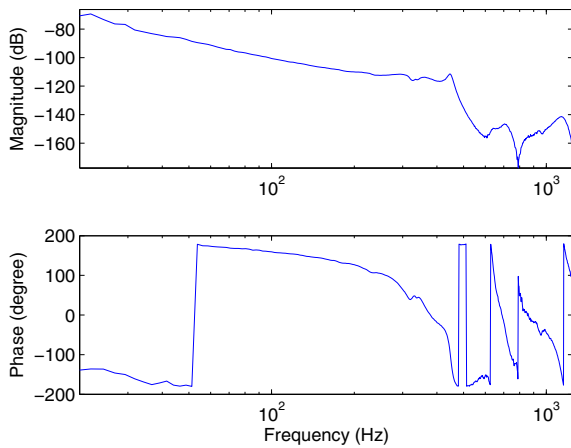


Fig. 3. Frequency response of the reticle stage

vibration compensation (where disturbance compensation is only turned on after detection of large errors).

## 2. SIMULATION AND EXPERIMENTAL SET UP

The experimental results in this paper are obtained on a testbed of a wafer scanner/stepper system shown in Fig. 2. Such systems are essential for photolithography in fabrication of integrated circuits in the semiconductor industry. There are two moving stages in the testbed, mounted on air bearings and actuated by epoxy-core linear permanent magnet motors. The stage positions are measured by laser interferometers. A LabVIEW real-time system with field-programmable gate array (FPGA) is used to execute the control commands. The frequency response of the upper reticle stage is shown in Fig. 3. The input and the output are respectively the motor voltage command and the position of the moving stage.

Additional evaluations are performed on a benchmark hard disk drive (HDD) simulation tool developed by IEEJ, Technical Committee for Novel Nanoscale Servo Control (2007), a technical committee consisting of both industrial and academic experts in the field. The benchmark has been frequently used in the disk drive community for algorithm verification and performance comparison.

Both the wafer stage and the HDD are typical examples of integrated control systems in mechatronics, where we commonly have integrator or mass-damper type of plant dynamics (recall Fig. 3), due to the working principles of motors and actuators.

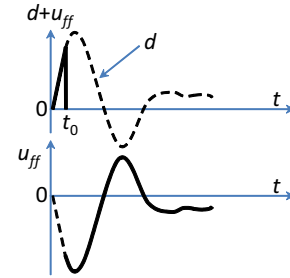


Fig. 4. Input discontinuity in UC for regulation control

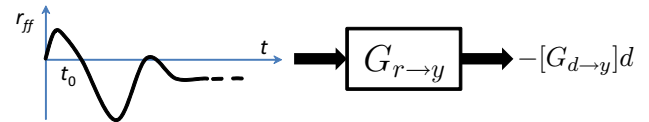


Fig. 5. Ideal UR disturbance compensation

## 3. TRANSIENT IN ADD-ON CONTROL

Consider cancellation of disturbances by UC feedforward control. Suppose the actual disturbance  $d$  is as shown in the top subplot in Fig. 4, where at time  $t_0$  the UC feedforward control is turned on. The ideal-case UC command  $u_{ff}$  is as shown in the solid line in the second subplot of Fig. 4, which perfectly cancels the disturbance after time  $t_0$ . The nature of the compensation scheme yields the abrupt change in the actual plant input  $d + u_{ff}$  at  $t_0$ , as: 1) strong external disturbances may not always present, and add-on compensation is turned on only when external disturbance reaches the threshold of violating the error tolerance; 2) the system can be subjected to different control tasks, where different disturbance properties require different add-on designs that necessitate new injection of the feedforward command.

The transient response under investigation is the response to the abrupt input discontinuity at  $t_0$ . The same discontinuity exists in disturbance compensation using add-on UR, where (recalling Fig. 1) we see that the effect of  $r_{ff}$  in the output should equal the negative of the disturbance effect  $[G_{d \to y}]d$ . Assume the ideal  $r_{ff}$  command is as shown in Fig. 5. Similar to the case in UC, when the plug-in control is switched on at time  $t_0$ , an input discontinuity is created. Fig. 6 presents the decomposition of the discontinuity, where  $r_{ff} = r_1 - r_2$ . The output w.r.t. the discontinuous  $r_2(t)$  will again create a transient response that depends on the dynamics of  $G_{r \to y}$  in Fig. 5.

Analogous analysis can be applied to the reference tracking problem. For instance, the combined reference input in UR will then have a discontinuity similar to that in Fig. 4.

## 4. PRACTICAL FEEDFORWARD INJECTION

In this section, formulations of feedforward-injection problems are provided for three common application schemes.

### 4.1 Two-degree-of-freedom control

Similar to Li and Tomizuka (1999); Sugie and Yoshikawa (1986); Liu et al. (2005), we refer to the basic combined

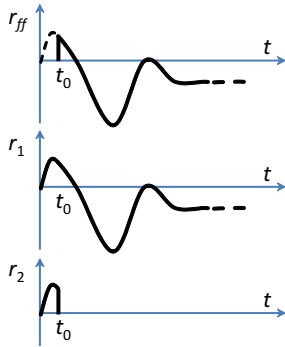


Fig. 6. Command decomposition in UR

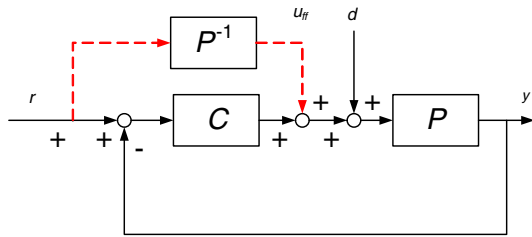


Fig. 7. 2DOF design with updated control feedforward

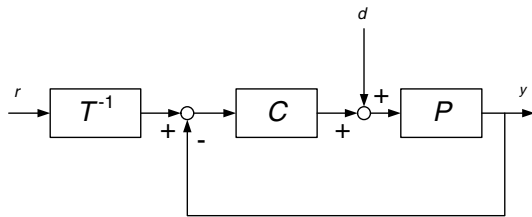


Fig. 8. 2DOF design with updated reference feedforward

control scheme using feedback and feedforward as two-degree-of-freedom (2DOF) control. Figs. 7 and 8 show the two structures of 2DOF configuration, respectively in the UC and UR schemes. In Fig. 7,

$$y = \left[ \frac{PC}{1+PC} \right] r + \left[ \frac{P}{1+PC} P^{-1} \right] r + \left[ \frac{P}{1+PC} \right] d \quad (1)$$

$$= \left[ \frac{PC}{1+PC} \right] r + \left[ \frac{P}{1+PC} \right] u_{ff} + \left[ \frac{P}{1+PC} \right] d \quad (2)$$

and in Fig. 8 we have

$$y = \left[ \frac{PC}{1+PC} T^{-1} \right] r + \left[ \frac{P}{1+PC} \right] d \quad (3)$$

$$= \left[ \frac{PC}{1+PC} \right] r + \left[ \frac{PC}{1+PC} \right] r_{ff} + \left[ \frac{P}{1+PC} \right] d \quad (4)$$

where  $r_{ff} = [T^{-1} - 1] r$ .

The condition of perfect reference tracking is that, the inverse model  $P^{-1}$  is perfect in (1) and  $T^{-1} = (1 + PC)/PC$  in (3). Under such conditions, if  $P^{-1}$  and  $T^{-1}$  are stable, then we can readily derive the steady-state equivalence between the two schemes, as  $T^{-1}$  equals  $1 + (PC)^{-1}$  after simplification, and updated reference is equivalent to updated error (recall Section 1), so that Fig. 8 is equivalent to Fig. 9, and hence to Fig. 7.

<sup>1</sup> In this paper, we use  $[G]r$  to represent the output of the transfer function  $G$  w.r.t. the input  $r$ .

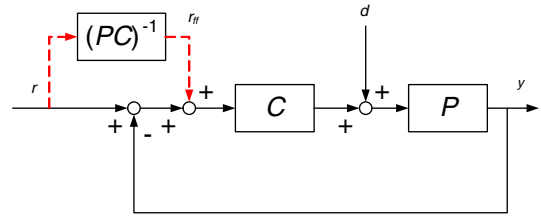


Fig. 9. Equivalent form of Fig. 8 if  $T^{-1}$  is perfect

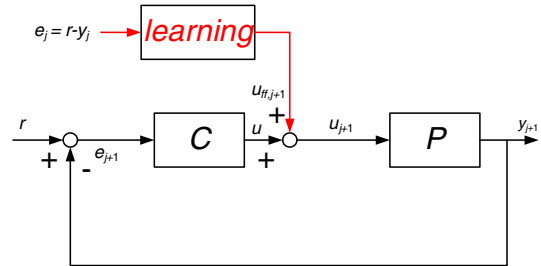


Fig. 10. Updated control ILC

We emphasize that despite the algebraic equivalence if  $T^{-1} = (1 + PC)/(PC)$ , in practice  $P^{-1}$  and  $T^{-1}$  are commonly not strictly stable. For building the approximate inverse  $P_{\text{approx}}^{-1}$  and  $T_{\text{approx}}^{-1}$ , it is common to do  $T_{\text{approx}}^{-1} = (T^{-1})_{\text{approx}}$ , namely,  $T^{-1}$  is considered as an entire filter to approximate, rather than a composition of  $T_{\text{approx}}^{-1} = (1 + P_{\text{approx}}C)/(P_{\text{approx}}C)$ . This is beneficial, for instance, when  $P$  has complicated dynamics itself but  $T$  (at least the desired shape of it) is simple, and hence  $T_{\text{approx}}^{-1}$  can have a low-order and often more robust realization.

A second remark is that, the equivalence between Fig. 7 and Fig. 9 holds only if the two dotted feedforward lines are always enabled together with the feedback controller  $C$ . If feedforward control is of *add-on* type, the transient behavior is not the same in the two schemes.

#### 4.2 Iterative Learning Control

Iterative learning control (ILC) is a standard technique in controlling repeated process (e.g., transportation of the workpieces in a product line in manufacturing). Using the errors made in the previous cycle of the process, ILC updates the control strategies as demonstrated in Fig. 10.<sup>2</sup> In this UC ILC scheme, manipulation is performed to the final control command:

$$u_{j+1} = u + u_{ff,j+1} = u + [Q] \{u_{ff,j} + [L] e_j\} \quad (5)$$

where  $j$  is the iteration number,  $L$  is the learning filter that extracts the desired information from the previous error  $e_j \triangleq r - y_j$ , and  $Q$  is the robustness filter to control the learning process.

The added  $u_{ff,j+1}$  affects the output by

$$y_{j+1} = \left[ \frac{PC}{1+PC} \right] r + \left[ \frac{P}{1+PC} \right] u_{ff,j+1} \quad (6)$$

The new errors can be shown to satisfy

<sup>2</sup> We focus on repeated tracking problems. ILC can also handle repeated disturbances. The analysis is analogous and omitted here.

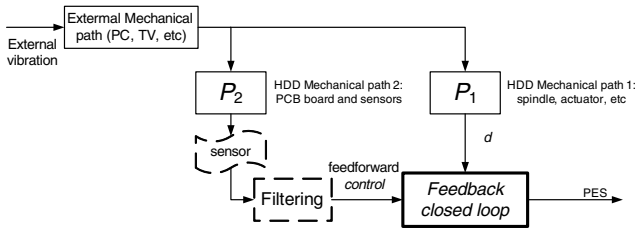


Fig. 11. Sensor-based feedforward control in HDDs

$$e_{j+1} = \left[ Q \left( 1 - L \frac{P}{1+PC} \right) \right] e_j + \left[ \frac{1-Q}{1+PC} \right] r \quad (7)$$

On the other hand, for UR ILC, the feedforward term is injected via

$$r_{j+1} = r + r_{ff,j+1} = r + [Q] \{ r_{ff,j} + [L] e_j \}$$

Analogous to UC ILC,

$$y_{j+1} = \left[ \frac{PC}{1+PC} \right] r + \left[ \frac{PC}{1+PC} \right] r_{ff,j+1} \quad (8)$$

and

$$e_{j+1} = \left[ Q \left( 1 - L \frac{PC}{1+PC} \right) \right] e_j + \left[ \frac{1-Q}{1+PC} \right] r \quad (9)$$

From (7) and (9), perfect learning is achieved by  $Q = 1$ ;  $L = [P/(1+PC)]^{-1}$  in UC ILC and  $L = [PC/(1+PC)]^{-1}$  in UR ILC. In both cases, the feedforward command is of add-on type, with iteration-dependent signal properties.

Comparing (2) with (6), and (4) with (8), we see that the 2DOF feedforward and ILC are structurally quite similar, and  $\{PC/(1+PC), P/(1+PC)\}$  are the two central transfer functions determining the transient and steady-state performances.

#### 4.3 Sensor-based Feedforward Disturbance Rejection

A significant issue in practical precision systems is to deal with large external disturbances. Such disturbances may come from expectable error sources in the working environment (e.g., the vibration of a HDD in a personal laptop playing loud music or movies), or unexpectedly as a shock disturbance to the system. The latter is a particularly important issue in advanced manufacturing, where the required working condition of the fabrication device is usually so demanding that a sudden shock may pause or even stop the manufacturing process.

In sensor-based feedforward compensation, motion sensing elements such as accelerometers are applied to measure the (expectable and unexpected) disturbances. Take the example of hard disk drive control. The sensor measurement detects the vibration reflected on the PCB board, which is correlated to the actual disturbance to the HDD actuator, as shown in Fig. 11. Feedforward design aims at generating the compensation signal to cancel the effect of the disturbance  $d$  on the position error signal (PES).

It is clear that the construction of feedforward should depend not only on  $P_1$  and  $P_2$ , but also on the location of feedforward control injection. Fig. 11 can be first simplified to the general block diagram in Fig. 12. Here the effect of the external vibration is lumped as an input disturbance to the closed loop, with the related dynamics explained by

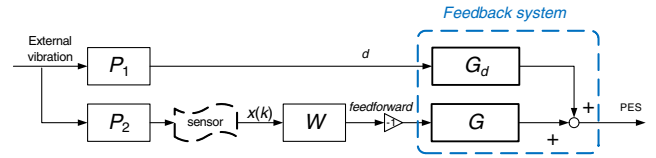


Fig. 12. Analysis form of Fig. 11

$G_d = P/(1+PC)$  (recall Fig. 1). The feedforward path applies a filter  $W$  to generate the compensation signal using the measured image of the external disturbance. Recall the two feedforward injection schemes in Fig. 1. Simple observation gives that the transfer function between the feedforward signal and PES, denoted as  $G$ , are respectively

	updated control	updated reference
$G$	$\frac{P}{1+PC}$	$\frac{PC}{1+PC}$

Ideally, to minimize PES, we need

$$G_d P_1 - G W P_2 = 0 \Leftrightarrow W = \frac{G_d P_1}{G P_2}$$

With  $G_d = P/(1+PC)$  and the above table of  $G$ , we have

	updated control	updated reference
$W$	$\frac{P_1}{P_2}$	$\frac{P_1}{C P_2}$

The above are the ideal-case feedforward controller structures, if the filters are stable and realizable in practice. Again, the steady-state performance is the same if  $W$  is correctly configured according to the aforementioned discussions, yet transient exists when feedforward is injected to the closed-loop in Fig. 12. The transient dynamics depends on the dynamics of  $G$ , namely  $P/(1+PC)$  in UC and  $PC/(1+PC)$  in UR.

## 5. TRANSIENT PERFORMANCE

Following the comparison and steady-state equivalence condition of UC and UR in Section 4, this section analyzes the transient performance of the two feedforward control allocation schemes. Let  $P = N_P/D_P$ ,  $C = N_C/D_C$ , where  $N_{\{\cdot\}}$  and  $D_{\{\cdot\}}$  denote respectively the numerator and denominator polynomials of a transfer function. Then

$$\frac{PC}{1+PC} = \frac{N_P N_C}{N_P N_C + D_P D_C} \quad (10)$$

$$\frac{P}{1+PC} = \frac{N_P D_C}{N_P N_C + D_P D_C} \quad (11)$$

It can be observed that the above transfer functions differ only in the location of the zeros. For the response to the signal discontinuities in Figs. 4 and 6, the pursued goal in this section is to show that (10) provides faster transient than (11) under a properly designed feedback loop.

We first note that in general motion control, the roots of  $N_C$  (i.e., zeros of  $C$ ) are always designed to be stable. Simple evaluation verifies this point in PID and lead-lag based controls. For instance, consider the PID controller

$$C(s) = k_p + k_i \frac{1}{s} + k_d s = \frac{k_p s + k_i + k_d s^2}{s} \quad (12)$$

where all the PID gains are positive. The Routh test reveals that all zeros of  $C(s)$  are stable  $\forall k_p > 0, k_i > 0, k_d > 0$ .

0. The same conclusion can be made for the causal version (for practical implementation) where  $C(s) = k_p + k_i \frac{1}{s} + k_d \frac{s}{\tau s + 1}$  ( $\tau$  is a small positive scalar). The above are for designs in the continuous-time domain. After discretization via bilinear transform  $s = 2(z - 1)/[T_s(z + 1)]$  ( $T_s$  is the sampling time), the left half of the  $s$  plane is mapped to the inside of the unit circle on the  $z$  plane, and the digital version of the controller preserves the stability of the zeros. Hence in both continuous- and discrete-time designs, the controller has stable zeros. Indeed, non-minimum-phase zeros of  $C$  (if there are any) will become non-minimum-phase zeros of the loop transfer function  $L = PC$ . From various fundamental limitations of feedback control (Doyle et al. (1992); Stein (2003)), open-loop unstable zeros will amplify the waterbed effect and place direct constraints on the achievable servo performance. Hence, unless really necessary,  $C$  should be designed to have stable zeros.

The situation is different for the roots of  $D_C$  (poles of  $C$ ). For the case of PID control in (12),  $C$  has a marginally stable pole. For lead-lag controllers, a stable pole close to the imaginary axis will occur due to the module of  $(s + b) / (s + a)$ . Actually, from basic frequency-response concepts, marginal poles at low frequencies are always needed for high-gain feedback to achieve good low-frequency servo.

It is well-known that stable zeros can accelerate the transient and unstable zeros reduce the speed of transient and can even introduce undesired undershoot in the step response. Hence from the design principles of the feedback loop, (10) is better than (11) from the viewpoint of transient performance. Indeed, (10) is the closed-loop complementary sensitivity function and the transfer function from the reference  $r$  to the output  $y$ . In any (linear and even nonlinear) feedback design, great efforts are made to make sure good tracking of  $r$  by  $y$ , both in the steady-state and the transient stages. While usually little or no direct attention is paid to the transient and steady-state performances of  $P/(1 + PC)$ . Hence from either the perspective of stable and unstable zeros, or fundamental goals of feedback design,  $PC/(1 + PC)$ , and hence UR feed-forward allocation, would have better and more consistent transient performance.

Next, validation and some additional design properties are provided via a practical example. Consider the plant  $P(s) = 1/(0.2556s^2 + 0.279s)$ , which is the nominal model of one stage of the wafer-scanner system in Section 2.

Closing the (negative) feedback loop with  $C(s) = 3000(1 + 2\frac{1}{s} + 0.012s)$  yields<sup>3</sup>

$$\frac{P(s)C(s)}{1 + P(s)C(s)} = \frac{36s^2 + 3000s + 6000}{0.2556s^3 + 36.279s^2 + 3000s + 6000}$$

$$\frac{P(s)}{1 + P(s)C(s)} = \frac{3.9124s}{(s + 2.05)(s^2 + 139.9s + 11450)} \quad (13)$$

Simple calculation reveals that  $PC/(1 + PC)$  has a stable pole at  $-2.05009$  and a stable zero at  $-2.05045$ . Hence after factorization

$$\frac{P(s)C(s)}{1 + P(s)C(s)} \approx \frac{140.8451(s + 81.28)}{s^2 + 139.9s + 1.145 \times 10^4} \quad (14)$$

<sup>3</sup> In implementation, the causal version  $s/(1 + \tau s)$  will replace the pure differentiation action.

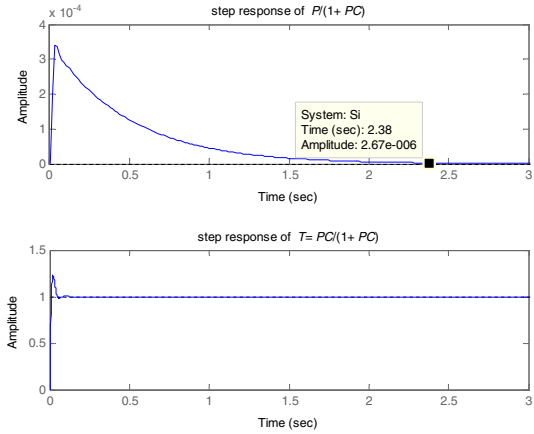


Fig. 13. Transient comparison: step response

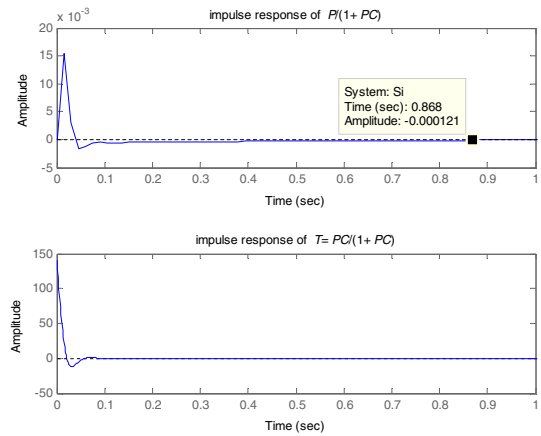


Fig. 14. Transient comparison: impulse response

Comparing the central transfer functions for updated reference (14) and updated control (13), we see that the slowly convergent mode  $e^{-2.05009t}$  (corresponding to the pole at  $-2.05009$ ) is firstly removed in (14), and hence accelerating the transient. Meanwhile, the marginally stable zero in (13) is replaced with a strictly stable one in (14). It is a standard result that such a zero improves the transient speed: for instance, from initial-value theorem, the step response of (14) has an initial slope of 140.8451 (assuming zero-initial conditions for  $P(s)$  and  $C(s)$ ) while the step response of (13) has a zero initial slope—much slower than the response of (14). Rigorous analysis using the theory of distributions can provide the mathematical expressions of different transient responses in (14) and (13). Limited by space, the results are omitted in this paper.

Figs. 13 and 14 compare the step and the impulse responses for  $P/(1 + PC)$  and  $PC/(1 + PC)$ . The results support the mathematical analysis: for both types of transient evaluation,  $PC/(1 + PC)$  has much shorter transients compared to  $P/(1 + PC)$ .

## 6. SIMULATION AND EXPERIMENTS

The analysis in preceding sections suggests that the same steady-state performance can be obtained in UC and

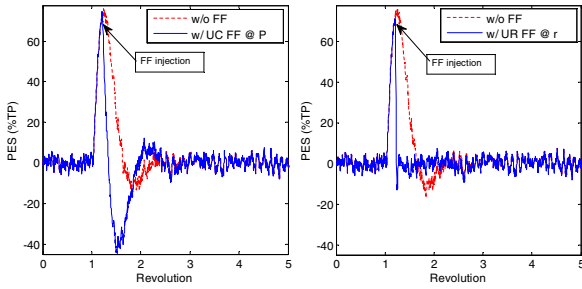


Fig. 15. Step-disturbance rejection performance

UR feedforward designs, and that UR provides better transient responses than UC. Certainly,  $T = PC/(1 + PC)$  also has a standard shape in feedback design (it is designed to approximate identity), and the shape of  $P/(1 + PC)$  is largely plant dependent. Such properties also make UR feedforward beneficial from the viewpoints of filter implementation and industrial mass production. This section validates the results with two application examples.

### 6.1 Simulated regulation control on a HDD

This example uses the HDD benchmark to verify the influence of feedforward allocations in regulation control. Here the reference is zero. A set of baseline disturbances consisting of white sensor noises, periodic disturbances from the disk rotations, and non-repeatable colored noises, is applied to the plant. For testing the transient performance with respect to shock resistance, we additionally applied (i) a step disturbance, and (ii) a half sinusoidal disturbance to the system. Both tests reveal the transient properties of the closed loop. In particular, (ii) is a standard testing procedure in HDD industry.

The overall control scheme is as shown in Fig. 12. The feedback controller in this case comes from the benchmark, which gives a baseline bandwidth of 1.19 kHz, a gain margin of 5.45 dB, and a phase margin of 38.2 deg. The dynamics  $P_1$  and  $P_2$  between the disturbance source and the HDD control loop are selected such that their ratio  $P_1/P_2$  matches that of experimental measurements provided in White (1997).

Figs. 15 and 16 show the transient difference in this sensor-based feedforward control. In Fig. 16, a step shock disturbance is injected at 1 sec. Although the sensor measurement is always turned on, in practical situations, the feedforward command is turned on after a disturbance detector reports large errors. In this simulation, a delay of 0.2 sec is used to mimic the effect of the disturbance detector. From the results in Fig. 15, the PES immediately reduces after turning on the feedforward compensation, and both algorithms performed well at steady state. The difference of the transient performance is however also self-explanatory. In UC feedforward (FF), the longer transient of  $P/(1 + PC)$  makes the settling time much longer than the case of UR FF. Similar observations can be made in the case of half-sinusoidal shock response in Fig. 16.

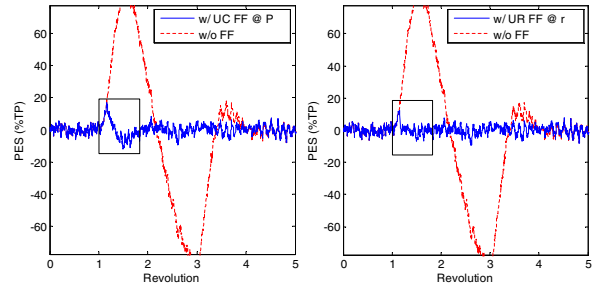


Fig. 16. Performance comparison for shock compensation

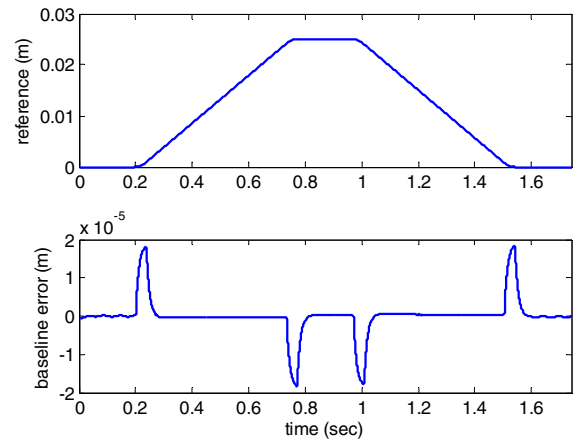


Fig. 17. Reference scanning trajectory and baseline tracking error without feedforward control

### 6.2 Experiments of tracking control on a wafer scanner

The second example compares the feedforward performance for combined 2DOF and ILC tracking control in the wafer scanner testbed. The reference scanning trajectory is as shown in the top plot of Fig. 17. Also shown in the figure is the baseline tracking result without feedforward control. After turning on the 2DOF feedforward control, the tracking error improved as shown in Fig. 18. The results indicate first, that both feedforward schemes significantly improves the tracking error—the maximum magnitude of the error in Fig. 17 is close to  $2 \times 10^{-5}$  m while in Fig. 18 it is about one magnitude smaller. Second, injection at the reference provides improved transient response—at the transition regions of the trajectory (at around 0.2 sec, 0.75 sec, 1 sec, and 1.5 sec), the UR feedforward with  $T^{-1}$  provides much smaller errors compared the UC feedforward with  $P^{-1}$ .

$T^{-1}$  and  $P^{-1}$  are both not strictly stable in this example, and approximated by ZPET method (Tomizuka, 1987), according to the remark at the end of Section 4.1. The bias in the error difference is due to the slight difference in the initial condition at time 0, and the fact that there is model uncertainty in the plant. Such bias is immediately removed in Fig. 19, where online ILC is applied and information from the physical plant (instead of just the models) comes into the learning scheme.

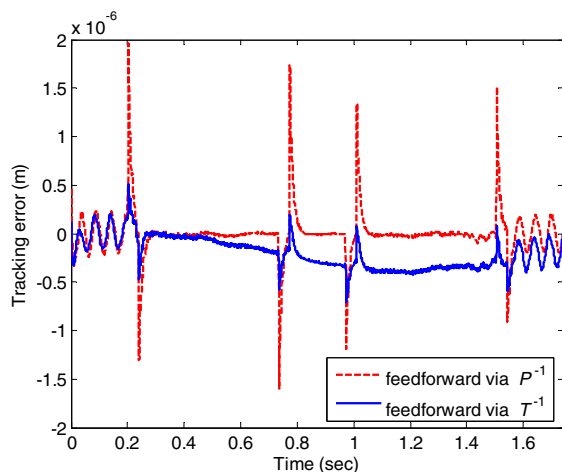


Fig. 18. Tracking errors with 2DOF feedforward schemes

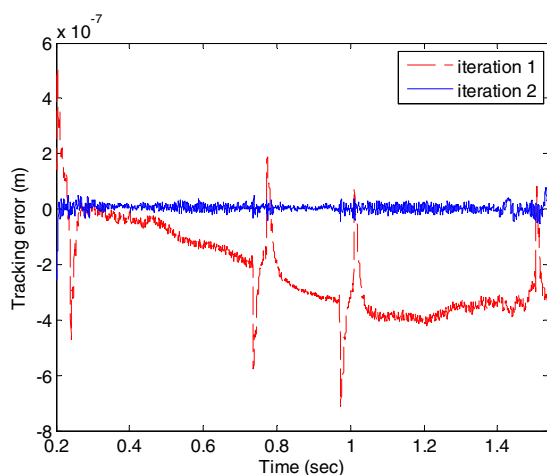


Fig. 19. Tracking error with UR ILC

## 7. CONCLUSION

In this paper, we have compared the performance differences between updated control and updated reference in feedforward design, and revealed the often neglected transient comparisons in feedforward control allocation. We have shown, via analysis of three common feedforward schemes, the conditions of steady-state equivalence, and the intrinsic faster transient performance in updated reference control. The results are general for motion control and mechatronics, and are important for various types of add-on feedforward designs.

## REFERENCES

Ahn, H.S., Chen, Y., and Moore, K.L. (2007). Iterative Learning Control: Brief Survey and Categorization. *IEEE Transactions on Systems, Man and Cybernetics, Part C (Applications and Reviews)*, 37(6), 1099–1121. doi:10.1109/TSMCC.2007.905759.

Amann, N., Owens, D.H., and Rogers, E. (1996). Iterative learning control using optimal feedback and feedforward actions. *International Journal of Control*, 65(2), 277–293.

Bodson, M., Sacks, a., and Khosla, P. (1994). Harmonic generation in adaptive feedforward cancellation

schemes. *IEEE Transactions on Automatic Control*, 39(9), 1939–1944. doi:10.1109/9.317130.

Bristow, D.A., Tharayil, M., and Alleyne, A. (2006). A survey of iterative learning control. *IEEE Control Systems Magazine*, 26(3), 96–114.

Doyle, J.C., Francis, B.A., and Tannenbaum, A. (1992). *Feedback control theory*. Macmillan.

IEEJ, Technical Committee for Novel Nanoscale Servo Control (2007). NSS benchmark problem of hard disk drive systems. <http://mizugaki.iis.u-tokyo.ac.jp/nss/>.

Li, Y. and Tomizuka, M. (1999). Two-degree-of-freedom control with robust feedback control for hard disk servo systems. *IEEE/ASME Transactions on Mechatronics*, 4(1), 17–24.

Liu, T., Zhang, W., and Gu, D. (2005). Analytical design of two-degree-of-freedom control scheme for open-loop unstable processes with time delay. *Journal of Process Control*, 15(5), 559 – 572.

Mishra, S. (2009). *Fundamental issues in iterative learning controller design: Convergence, robustness, and steady state performance*. Ph.D. dissertation, University of California, Berkeley.

Moore, K.L., Ahn, H.s., and Chen, Y. (2008). Iteration domain H-infinity optimal iterative learning controller design. *International Journal of Robust and Nonlinear Control*, (May 2007), 1001–1017. doi:10.1002/rnc.

Moore, K.L., Chen, Y., and Ahn, H.S. (2006). Iterative Learning Control: A Tutorial and Big Picture View. *Proc. 45th IEEE Conf. on Decision and Control*, (Ilc), 2352–2357. doi:10.1109/CDC.2006.377582.

Nie, J. and Horowitz, R. (2011). Control design of hard disk drive concentric self-servo track writing via  $h_2$  and  $h_\infty$  synthesis. *IEEE Transactions on Magnetics*, 47(7), 1951–1957. doi:10.1109/TMAG.2011.2125948.

Saab, S. (1994). On the P-type learning control. *IEEE Transactions on Automatic Control*, 39(11), 2298–2302.

Stein, G. (2003). Respect the unstable. *IEEE Control Systems*, 23(4), 12 – 25. doi:10.1109/MCS.2003.1213600.

Sugie, T. and Yoshikawa, T. (1986). General solution of robust tracking problem in two-degree-of-freedom control systems. *Automatic Control, IEEE Transactions on*, 31(6), 552–554. doi:10.1109/TAC.1986.1104337.

Tomizuka, M. (1987). Zero phase error tracking algorithm for digital control. *ASME Journal of Dynamic Systems, Measurements, and Control*, 109(1), 65–68.

White, M.T. (1997). *Control techniques for increased disturbance rejection and tracking accuracy in magnetic disk drives*. Ph.D. dissertation, University of California, Berkeley.

Widrow, B. and Walach, E. (2007). *Adaptive Inverse Control, Reissue Edition: A Signal Processing Approach*. Wiley-IEEE Press.

Zhang, J., Chen, R., Guo, G., and Low, T.s. (2000). Modified adaptive feedforward runout compensation for dual-stage servo system. *IEEE Transactions on Magnetics*, 36(5), 3581–3584. doi:10.1109/20.908908.